

Development of 0.5-V Josephson junction array devices for quantum voltage standards

Lanruo Wang(王兰若), Jinjin Li(李劲劲), Wenhui Cao(曹文会), Yuan Zhong(钟源), Zhonghua Zhang(张钟华)

Citation: Chin. Phys. B . 2019, 28(6): 068501. **doi:** 10.1088/1674-1056/28/6/068501
Journal homepage: http://cpb.iphy.ac.cn; http://iopscience.iop.org/cpb

What follows is a list of articles you may be interested in

Characterization of barrier-tunable radio-frequency-SQUID for Maxwell's demon experiment

Gang Li(李刚), Suman Dhamala, Hao Li(李浩), Jian-She Liu(刘建设), Wei Chen(陈炜)

Chin. Phys. B . 2018, 27(6): 068501. **doi:** 10.1088/1674-1056/27/6/068501

Modulation depth of series SQUIDs modified by Josephson junction area

Jie Liu(刘杰), He Gao(高鹤), Gang Li(李刚), Zheng Wei Li(李正伟), Kamal Ahmada, Zhang Ying Shan(张颖珊), Jian She Liu(刘建设), Wei Chen(陈炜)

Chin. Phys. B . 2017, 26(9): 098501. **doi:** 10.1088/1674-1056/26/9/098501

Bridge-free fabrication process for Al/AlO$_x$/Al Josephson junctions

Ke Zhang(张珂), Meng-Meng Li(李蒙蒙), Qiang Liu(刘强), Hai-Feng Yu(于海峰), Yang Yu(于扬)

Chin. Phys. B . 2017, 26(7): 078501. **doi:** 10.1088/1674-1056/26/7/078501

Fabrication of Al/AlO$_x$/Al junctions using pre-exposure technique at 30-keV e-beam voltage

Dong Lan(兰栋), Guangming Xue(薛光明), Qiang Liu(刘强), Xinsheng Tan(谭新生), Haifeng Yu(于海峰), Yang Yu(于扬)

Chin. Phys. B . 2016, 25(8): 088501. **doi:** 10.1088/1674-1056/25/8/088501

Increasing energy relaxation time of superconducting qubits with nonmagnetic infrared filter and shield

Yuhao Liu(刘宇浩), Mengmeng Li(李蒙蒙), Dong Lan(兰栋), Guangming Xue(薛光明), Xinsheng Tan(谭新生), Haifeng Yu(于海峰), Yang Yu(于扬)

Chin. Phys. B . 2016, 25(5): 058501. **doi:** 10.1088/1674-1056/25/5/058501

Development of 0.5-V Josephson junction array devices for quantum voltage standards*

Lanruo Wang(王兰若)[1], Jinjin Li(李劲劲)[2,3,†], Wenhui Cao(曹文会)[2,3], Yuan Zhong(钟源)[2,3], and Zhonghua Zhang(张钟华)[2,3]

[1] *Department of Electrical Engineering, Tsinghua University, Beijing* 100089, *China*
[2] *National Institute of Metrology, Beijing* 122000, *China*
[3] *Key Laboratory of the Electrical Quantum Standard of AQSIQ, Beijing* 122000, *China*

(Received 22 November 2018; revised manuscript received 27 March 2019; published online 8 May 2019)

The design, fabrication, and the characterization of a 0.5-V Josephson junction array device are presented for the quantum voltage standards in the National Institute of Metrology (NIM) of China. The device consists of four junction arrays, each of which has 1200 3-stacked Nb/Nb$_x$Si$_{1-x}$/Nb junctions and an on-chip superconducting microwave circuit which is mainly a power divider enabling each Josephson array being loaded with an equal amount of microwave power. A direct current (dc) quantum voltage of about 0.5 V with a $\sim$ 1-mA current margin of the 1st quantum voltage step is obtained. To further prove the quality of NIM device, a comparison between the NIM device with the National Institute of Standards and Technology (NIST) programmable Josephson voltage standard (PJVS) system device is conducted. The difference of the reproduced 0.5-V quantum voltage between the two devices is about 0.55 nV, which indicates good agreement between the two devices. With the homemade device, we have realized a precise and applicable 0.5-V applicable-level quantum voltage.

Keywords: Josephson voltage standards, Josephson junction, superconducting-normal metal–superconducting (SNS) junction, quantum device

PACS: 85.25.Cp, 74.81.Fa, 06.20.fa, 84.37.+q **DOI:** 10.1088/1674-1056/28/6/068501

1. Introduction

Since the 1990s, the high-stable non-hysteresis Josephson junction (JJ) has been widely used in quantum voltage standards because of its accurate and stable Shapiro voltage step. The integrated Josephson junction array device is the core element of direct current (dc) and alternating current (ac) quantum voltage standards. Josephson voltage standard devices of 1 V and 10 V have been developed in National Institute of Standards and Technology (NIST), Physikalisch-Technische Bundesanstalt (PTB), and National Metrology Institute of Japan (NMIJ). In NIST, 10-V devices have been realized using about 2.6×10^5 Nb/Nb$_x$Si$_{1-x}$/Nb superconducting-normal-superconducting (SNS) Josephson junctions, and the current margin for the 1st voltage step can reach 2 mA with 18 GHz$\sim$20 GHz microwave irradiation.[1–4] In 2010, together with NIST, PTB realized an output of 10-V quantum voltage with voltage step width of more than 1.5 mA using 69632 SNS junctions operating at 70 GHz.[5–7] Using about 2.5×10^5 NbN/TiN/NbN Josephson junctions, NMIJ also achieved 10-V voltage output with about 0.8-mA current margin. The device yield is about 36%.[8,9] Josephson arbitrary waveform synthesizer (JAWS), which is also known as ac Josephson voltage standard, has caused widespread concern because of its advantages in synthesizing signal with higher frequency in broadband widths. Recently, two 1-V JAWS chips are combined on a cryocooler to generate a 2-V system, and a 1.6-mA operating current margin is observed in NIST.[10]

For many years, the National Institute of Metrology (NIM) of China has been developing large-scale integrated Josephson junction array devices that are the basis for the quantum voltage standard.[11–13] The primary challenge has been to increase the output voltage, which depends on improvements and innovations on circuit design and fabrication process control. In this paper, we present the design, fabrication, and the characterization of a 0.5-V Josephson junction array device for the quantum voltage standard. A tapered transmission line is designed, which is focused on the consideration of dissipative characteristics of Josephson junctions. A whole fabrication process control is conducted and several key steps are improved to improve the performance of our devices. High-quality Nb film deposition technology is explored and the optimal conditions of film sputtering can be found in our previously published paper.[14] In addition, multi-stacked Josephson junctions vertical etching technology, crystal plane fracture in microstructure, and phase shifter configurations in power divider circuits are also researched and improved. Using about 14400 Nb/Nb$_x$Si$_{1-x}$/Nb junctions, 0.516-V applicable-level quantum voltage with a 1.1-mA current

*Project supported by the National Key Research and Development Program of China (Grant No. 2016YFF02000402).
†Corresponding author. E-mail: jinjinli@nim.ac.cn
© 2019 Chinese Physical Society and IOP Publishing Ltd

margin of the 1st quantum voltage step has been achieved. To further prove the quality of NIM device, we compare the NIM device with NIST programmable Josephson voltage standard (PJVS) device, and a good consistency is obtained. The difference of the reproduced 0.5-V quantum voltage between the two devices is about 0.55 nV, which indicates that the NIM device can be applied to accurately reproduce the quantum voltage.

The rest of this paper is structured as follows. The design and fabrication processes are described in Section 2. The dc and ac *I*–*V* characteristics are presented in Section 3. The comparison of output voltages between NIM 0.5-V device and NIST 10-V PJVS device is expressed in Section 4. Finally, the conclusion of this work is given in Section 5.

2. Design and fabrication

2.1. Josephson voltage standard (JVS) circuits

A schematic diagram of basic circuit for 0.5-V JVS device is shown in Fig. 1. The device consists of four junction arrays and on-chip superconductor microwave circuits. Each junction array contains 1200 3-stacked Josephson junctions, and the four arrays are connected in series to obtain a total of 14400 JJs. The area of junction is 10 μm×6 μm. The microwave circuit mainly consists of Wilkinson microwave power dividers,[3,15] filters, transmission lines, *etc*. In our device, broadband two-stage lumped Wilkinson power dividers have been applied to split 1-way input microwave power into four ways. The microwave power is conducted using coplanar waveguide (CPW) transmission lines, with embedded Josephson junctions.

For SNS Josephson junction, microwave power loss may occur under microwave irradiation during working process. Thus, in a large-scale series integrated Josephson array, less microwave power will be received by the end of junction compared to the beginning of array, which will affect the consistency of the Josephson response of junctions in series. Meanwhile, self-emitting power will also be found in Josephson junctions in previous studies.[16,17]

A tapered transmission line makes a compensation on the attenuation effects of junctions, and the constant microwave current is the compensation target to keep the amplitude of microwave currents received by each junction to be constant. This compensation target is realized in circuit design by continuously adjusting characteristic impedance of transmission line with a comprehensive consideration of beginning characteristic impedances, stable resistance of junction, Josephson junction number n, and a correction factor considering self-emission effect of Josephson junction and mismatch in microwave circuit, and so on. Empirical data from our previous measurements and these parameters ranges also take into account the influences of differences caused by fabrication process.

A tapered transmission line with continuously decreasing characteristic impedance from 50 Ω to 40 Ω is used so that each junction receives nearly the same amount of microwave power. Low-pass filters with planar spiral inductor and paralleled resistance are used to apply dc signal and block microwave power. High frequency structure simulator (HFSS) simulations show that the return loss of the power divider is below 0.16 dB at 15 GHz∼ 22 GHz, and almost equal microwave power division is obtained with each array getting a division of 4.9 ± 0.4 dB of the total microwave power at 15 GHz∼ 22 GHz.

The coils at the end of each sub-arrays are designed as dc bias and low pass filters that can be realized by resister shunted spiral coil inductors, which can prevent resonances on a broadband signal ranges.

The multi-stage 2-way broadband Wilkinson power divider is designed to realize a π-model equivalent lumped-element that is suitable for on-chip fabrication and decrease physical dimension compared with distributed-elements. The designs are all simulated with Ansoft HFSS and advanced design system.

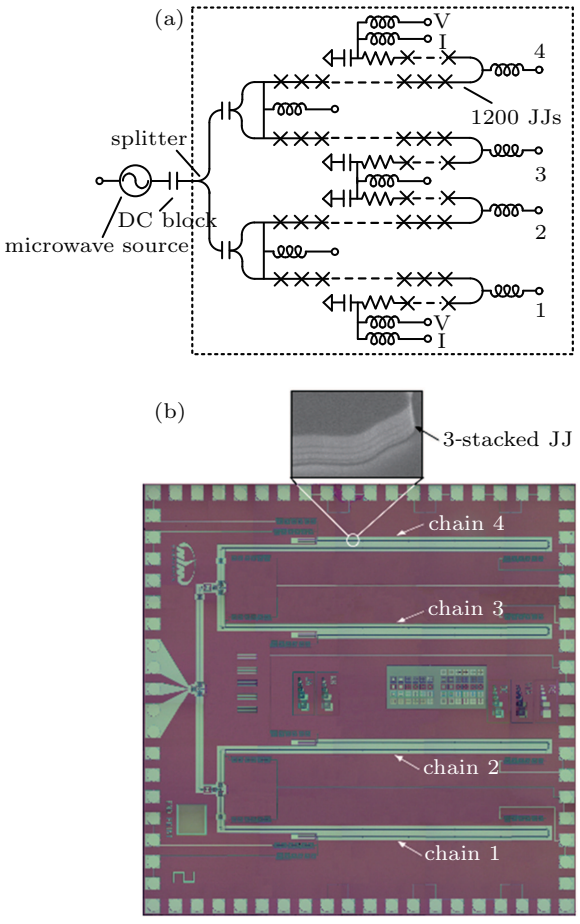


Fig. 1. Schematic diagram of a 0.5-V JVS device. (a) Circuit of the 0.5-V JVS device. (b) The image of the 0.5-V device under an optical microscope (1 cm×1 cm).

2.2. Fabrication process

The optical image of the fabricated device is shown in Fig. 1(b). The typical JVS device fabrication process in NIM is as follows. First, the stacked Nb/Nb_xSi_{1-x}/Nb sandwich layers are deposited with a magnetron sputtering system with a base pressure of about 2×10^{-8} Torr (1 Torr $\approx 1.33322 \times 10^2$ Pa). The substrate is a silicon wafer with a thin dioxide layer on it. The Nb_xSi_{1-x} barrier layer is deposited using a co-sputter scheme. Photolithography and reactive ion etching methods are used to define junction and electrode areas. Then, a SiO_2 insulating layer is deposited by plasma enhanced chemical vapor deposition. Vias are defined and etched. Next, Nb wiring layer is sputtered to form the on-chip superconducting microwave circuit. Finally, a PdAu resistance layer is deposited by electron beam evaporation. Detailed fabrication process can be found in our previously published paper.[11,13]

Another noteworthy point is that film stress will be accumulated during multi-layer fabrication, which may lead to a low current capacity of the devices. Crystal fractures in the Nb wiring layers are found in devices with poor current capacity, and we adjust the film stress of sandwich layer into compressive to improve stress accumulation effect, which can effectively improve the current capacity.

3. Measurement

The package of 0.5-V JVS device consists of a printed circuit board (PCB), a flexible printed circuit (FPC) interconnected board, and the device. The device sits on a copper pedestal which is a good heat sink and can rapidly dissipate the heat induced by the device to the 4.2-K helium liquid. The CPW transmission line on PCB is simulated and optimized by Ansoft HFSS and advanced design system (ADS). All connecting fingers and transmission lines on the PCB are gold-plated to enhance solderability and at the same time keep the capability of transmitting high frequency signals with low loss. We use sub-miniature version A (SMA) socket as coax-cryopackage connector. The packaged device is mounted at the end of cryo-probe and measured in a 100-L liquid helium Dewar at 4.2 K. A programmable multi-channel current source with high precision and low noise is used to bias junction arrays and an Aglient 33420A digital nano-voltmeter is used to measure the output voltage.

We first measure the dc I–V curve of the array. The critical current $I_c = 7.56$ mA and characteristic voltage $V_c = I_cR_n = 43.86$ μV. The ac I–V characteristics are then obtained under 17.46 GHz and 2-dBm microwave irradiation, as shown in Fig. 2. Figure 2(a) shows the ac I–V curves of the total arrays and figure 2(c) shows that of each array. We can see that the characteristics of the four sub-arrays are almost identical, which indicates that the designed on-chip superconducting circuits work well. Figure 2(b) shows the enlarged 1st quantum voltage step. The width of the step is 1.1 mA. Clearly, the step is very flat and satisfies the requirement of the quantum voltage standard. To increase the signal to noise ratio, we take the measurement for 10 times with the same microwave frequency and power to do the average. The averaged values of the 1st voltage steps of each sub-array are shown in the enlarged image in Fig. 2(d). The quantum voltage from chain 1, 3, and 4 is about 0.129976 V, while that from chain 2 is 0.129759 V, due to the presence of two shorted triple-stacked junctions (6 JJs) in chain 2. Thus, the total quantum voltage obtained at 17.46 GHz is about 0.519686 V (14394 JJs).

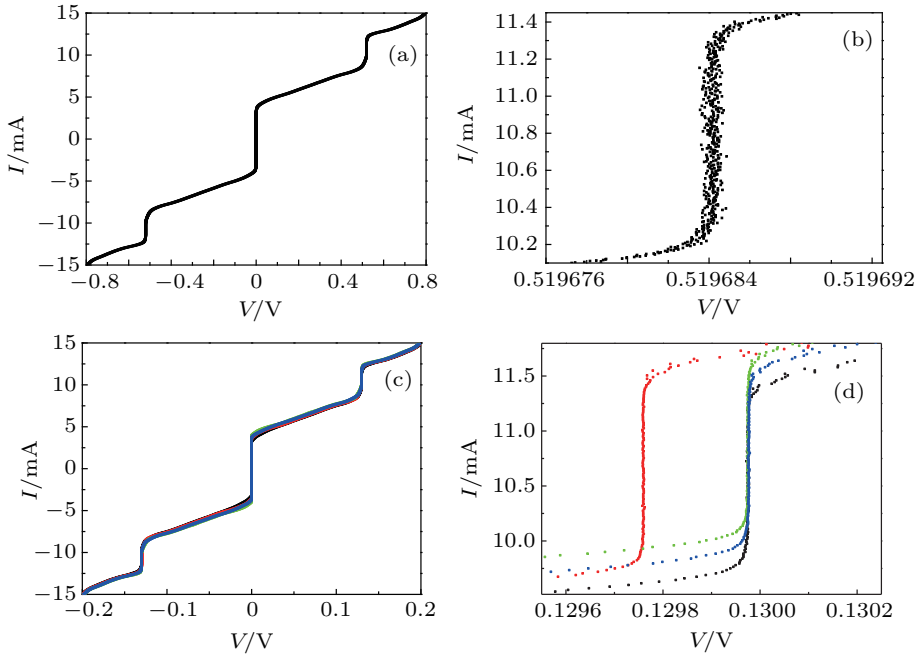


Fig. 2. (a) The ac I–V curves of the total array (14394 JJs) at 17.46 GHz. (b) The enlarged 1st quantum voltage step of panel (a). (c) The ac I–V curves of each of the four sub-arrays. (d) The enlarged 1st quantum voltage step of panel (c).

Further experiments show that a 0.583-V voltage can be achieved at 19.6 GHz, but the step width is reduced to about 0.8 mA. One reason to explain this is that thermal effects may be caused at high frequency and microwave power in large-scale integrated junction arrays. Further design will improve the heat dissipation performance both in device circuits and packages.

To fully examine the characteristics of the device, we check the ac I–V characteristics for each sub-array, not only on a fixed microwave frequency but also on a frequency range from 15 GHz to 20 GHz. Figure 3 shows the width of the 1st quantum voltage step as a function of microwave frequency. The microwave power is maintained at 20 dBm (without microwave power amplifier) during the measurement. It is clearly shown that oscillations exist which might be due to the oscillation of the bias circuit. The oscillation patterns of the four sub-arrays are very similar.

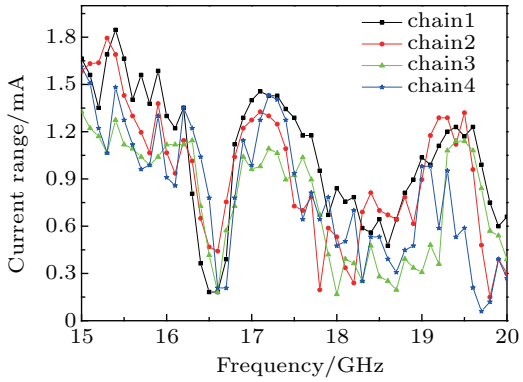


Fig. 3. The 1st step current range as a function of frequency from 15 GHz to 20 GHz for the four sub-arrays.

4. Voltage comparison between NIM 0.5-V device and NIST 10-V PJVS

To further verify the quality of the 0.5-V JVS device, we compare the NIM device with NIST PJVS device. The comparison method used is the so-called direct comparison where the two devices are biased at the same voltage, the outputs are connected in series opposition, and the two output voltages are compared directly. A schematic diagram of the comparison method is given in Fig. 4. The detailed procedure is described as follows. The NIM 0.5-V device and NIST 10-V PJVS are first biased at 0.465529813 V, which are marked as $V_{\mathrm{NIM\ 0.5\ V}}$ and $V_{\mathrm{NIST\ 10\ V}}$. For NIM device, 12894 JJs are connected in series to generate 0.465529813-V quantum voltage with 17.46-GHz microwave radiation. Then, a digital zero gauge is used to measure the differences between the two quantum voltage outputs.

A total of 20 measurements between the two systems are conducted and the results are shown in Fig. 5. The average value of 20 measurements and the corresponding uncertainty value are

$$\Delta V = V_{\mathrm{NIM\ 0.5\ V}} - V_{\mathrm{NIST\ 10\ V}} = 0.55\ \mathrm{nV}, \quad u = 1.6\ \mathrm{nV}. \quad (1)$$

The difference of the reproduced quantum voltage between the two devices is 0.55 nV, which indicates good agreement between the two devices. The combined standard uncertainty u, which includes both type-A and type-B uncertainty (system error), is 1.6 nV. Therefore, the NIM 0.5-V JVS device is capable of reproducing the applicable-level 0.5-V quantum voltage accurately.

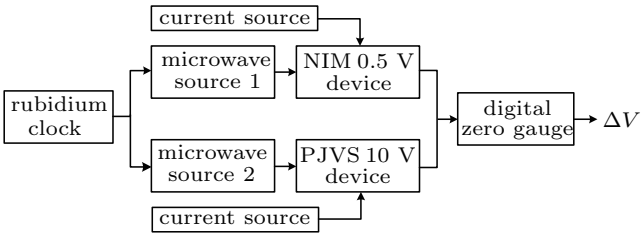


Fig. 4. Schematic diagram of voltage comparison method between $V_{\mathrm{NIM\ 0.5\ V}}$ and $V_{\mathrm{NIST\ 10\ V}}$.

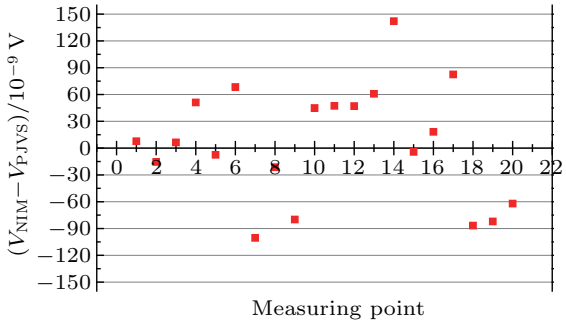


Fig. 5. Measurement results of 20 comparisons between $V_{\mathrm{NIM\ 0.5\ V}}$ and $V_{\mathrm{NIST\ 10\ V}}$. The difference of the reproduced quantum voltage between the two devices is 0.55 nV, with a 1.6-nV uncertainty.

5. Conclusion

In this paper, we present the design, fabrication, and characterization of NIM 0.5-V JVS device which is based on the Nb/Nb$_x$Si$_{1-x}$/Nb SNS junction technology. A quantum voltage of 0.519686 V with a 1.1-mA current margin is produced with a 3-stacked Josephson junction array under 17.46-GHz microwave radiation. To further prove the quality of NIM device, we compare the NIM device with the NIST PJVS. The difference of the reproduced 0.5-V quantum voltage between the two devices is 0.55 nV, which indicates good agreement between them. These results also verify the validity of our on-chip superconducting microwave circuit design, which can be applied to higher voltage devices in the future.

Acknowledgement

We thank Li Honghui, Wang Zengmin for the technical assistance and Zhong Qing, Wang Xueshen for the helpful discussion.

References

[1] Dresselhaus P D, Elsbury M M, Olaya D, Burroughs C J and Benz S P 2011 *IEEE Trans. Appl. Supercond.* **21** 693

[2] Dresselhaus P D, Elsbury M, Burroughs C J, Olaya D, Benz S P, Bergren N F, Schwall R and Popovic Z 2008 *Conference on Precision Electromagnetic Measurements Digest*, June 8–13, 2008, Broomfield, USA, pp. 102–103

[3] Elsbury M M, Dresselhaus P D, Benz S P and Popovic Z 2009 *IEEE MTT-S International Microwave Symposium Digest*, June 6–12, 2009, Boston, USA, pp. 997–1000

[4] Fox A, Dresselhaus P, Rufenacht A, Sanders A and Benz S 2015 *IEEE Trans. Appl. Supercond.* **25** Issue 3

[5] Mueller F, Behr R, Weimann T, Palafox L, Olaya D, Dresselhaus P D and Benz S P 2009 *IEEE Trans. Appl. Supercond.* **19** 981

[6] Behr R, Kieler O, Kohlmann J, Mueller F and Palafox L 2012 *Meas. Sci. Technol.* **23** 124002

[7] Kohlmann J, Mueller F, Kieler O, Behr R, Palafox L, Kahmann M and Niemeyer J 2007 *IEEE Trans. Instrum. Meas.* **56** 472

[8] Yamamori H, Yamada T, Sasaki H and Shoji A 2008 *Supercond. Sci. Technol.* **21** 105007

[9] Yamamori H, Yamada T, Sasaki H and Shoji A 2010 *IEEE Trans. Appl. Supercond.* **20** 71

[10] Flowers-Jacobs N E, Fox A E, Dresselhaus P D, Schwall R E and Benz S P 2016 *IEEE Trans. Appl. Supercond.* **26** 140020

[11] Cao W, Li J, Zhong Y, Gao Y, Li H, Wang Z and He Q 2016 *Chin. Phys. B* **25** 057401

[12] Wang L, Zhong Y, Li J, Qu J, Zhong Q, Cao W, Wang X, Zhou Z, Fu K and Shi Y 2018 *Acta Phys. Sin.* **67** 108501 (in Chinese)

[13] Cao W, Li J, Zhong Y and He Q 2015 *Chin. Phys. B* **24** 127402

[14] Wang L, Zhong Y, Li J, Cao W, Zhong Q, Wang X and Li X 2018 *Mater. Res. Express* **5** 046410

[15] Elsbury M M, Dresselhaus P D, Bergren N F, Burroughs C J, Benz S P and Popovic Z 2009 *IEEE Trans. Microwave Theory Tech.* **57** 2055

[16] Schulze H, Behr R, Muller F and Niemeyer J 1998 *Appl. Phys. Lett.* **73** 996

[17] Hassel J, Grönberg L, Helistö P and Seppä H 2006 *Appl. Phys. Lett.* **89** 072503